Off-shell behavior of the in-medium nucleon-nucleon cross section

C. Fuchs,[1] Amand Faessler,[1] and M. El-Shabshiry[2]
[1]*Institut für Theoretische Physik, Universität Tübingen, Tübingen, Germany*
[2]*Physics Department, Faculty of Science, Ain Shams University, Cairo, Egypt*
(Received 26 February 2001; published 6 July 2001)

The properties of nucleon-nucleon scattering inside dense nuclear matter are investigated. We use the relativistic Brueckner-Hartree-Fock model to determine on-shell and half off-shell in-medium transition amplitudes and cross sections. At finite densities the on-shell cross sections are generally suppressed. This reduction is, however, less pronounced than found in previous works. In case the outgoing momenta are allowed to be off energy shell the amplitudes show a strong variation with momentum. This description allows one to determine in-medium cross sections beyond the quasiparticle approximation, accounting thereby for the finite width which nucleons acquire in the dense nuclear medium. For reasonable choices of the in-medium nuclear spectral width, i.e., $\Gamma \leqslant 40$ MeV, the resulting total cross sections are, however, reduced by not more than about 25% compared to the on-shell values. Off-shell effects are generally more pronounced at large nuclear matter densities.

DOI: 10.1103/PhysRevC.64.024003 PACS number(s): 21.30.−x, 21.65.+f, 24.10.Cn

I. INTRODUCTION

One major topic of modern nuclear physics is the investigation of hadron properties inside a dense hadronic environment which exists, e.g., in the interior of neutron stars or is transiently created in energetic heavy ion collisions. In the latter case, the theoretical framework to describe the time evolution of heavy ion reactions is provided by kinetic transport theory. Starting from the quantum theory of strongly interacting Fermi systems, formulated within the framework of the Dyson-Schwinger hierarchy of nonequilibrium many-body Green functions [1], one can derive semiclassical transport equations of a Boltzmann-Uehling-Uhlenbeck (BUU) type [2,3]. These transport equations describe successfully the time evolution of a nonequilibrated strongly interacting hadron gas. To mention only the essential steps of such a derivation there are the truncation of the many-body hierarchy at the two-body level, a Wigner transformation of the density matrices with subsequent gradient expansion up to first order in $\hbar$, and the use of the quasiparticle approximation (QPA) which neglects the finite decay width of the particles. The resulting BUU equation consists of two parts, a drift term which propagates the particles dressed by the surrounding medium in a self-consistent mean field and the collision term responsible for binary nucleon-nucleon scattering. In a consistent treatment both ingredients—namely, the mean field and the binary cross sections—should be treated on the same footing, which means to base both of them on the same effective interaction. Unfortunately, in most applications to heavy ion collisions this is not done. The self-consistent mean field accounts for medium effects by its density dependence. For the cross section, on the other hand, the free (vacuum) expressions are widely used in transport calculations. It has, however, been noticed that in particular at incident energies below particle production thresholds, medium modifications of the cross sections can play an important role for the reaction dynamics in heavy ion collisions [4–6].

The relativistic (Dirac-)Brueckner approach [7–13] provides a powerful tool to achieve such a consistent description. Starting from free nucleon-nucleon interactions, given in its modern form by one-boson-exchange potentials [14], one treats the two-body correlations in dense nuclear matter in the ladder approximation of the Bethe-Salpeter equation. As a result the nuclear matter saturation properties are quite well described. This is achieved without the adjustment of additional parameters, such as, e.g., done in relativistic mean field models [15]. On the level of the T-matrix approximation both ingredients for the BUU equation follow from the on-shell in-medium T matrix (or G matrix). The mean field is determined by the real part Re T of the T matrix whereas the cross section $\sigma \simeq |T|^2$ is connected to the imaginary part Im T via an optical theorem [3]. Medium modifications arise due to the dressing of the quasiparticles and the existence of the Pauli operator which prevents the scattering of intermediate states in the Bethe-Salpeter equation (not final states) into occupied phase space areas. Both aspects are most pronounced at high densities and/or low momenta and lead to a suppression of the in-medium cross section compared to the free one.

There have already been several studies devoted to the in-medium NN scattering problem. The Tübingen group [4] and later the Rostock group [16,17] derived in-medium cross sections within the nonrelativistic Brueckner approach, in the latter case also at finite temperature. Relativistic calculations were performed in [18–20]. The most complete study of in-medium NN scattering within the Dirac-Brueckner approach was probably done by Li and Machleidt [21] who used the Bonn potentials as the bare interaction. Unfortunately the different approaches have led to partially contradictory results, in particular between relativistic [18,21] and nonrelativistic calculations [4]. Therefore, in the first part of this paper we reexamine the problem of on-shell scattering. The results are obtained with the Bonn A potential. In large parts we find good agreement with the previous investigations of Li and Machleidt [21]. However, their treatment [21] seems to overestimate the suppression of the in-medium cross section at low energies compared to the vacuum case.

The second part of this paper is devoted to an additional aspect: Kinetic transport equations are essentially based on the QPA which puts the nucleons on mass shell. The same holds in the medium for dressed quasiparticles. If the imaginary part of the nucleonic self-energy is negligible ($\mathrm{Im}\,\Sigma \ll \mathrm{Re}\,\Sigma$), the quasiparticle approximation as the zero-width limit ($\Gamma \propto \mathrm{Im}\,\Sigma$) for the nucleon spectral function appears to be justified [3]. However, it is well known that the spectral widths of hadrons change in the medium. It has further been pointed out that in the medium also ''stable'' particles can obtain a nonzero width, depending on their collision rates (collisional broadening); see, e.g., [22]. Following the work of Botermans and Malfliet [3] there have been several attempts to derive transport equations for nonequilibrated Fermi systems beyond the quasiparticle approximation; see [22–25] and references therein. However, as a result of the complications which arise giving up the QPA, these transport equations were never used in practical applications to heavy ion reactions but stayed more or less on the level of academic considerations. Just very recently there have been successful attempts to formulate generalized transport equations which can be handled in applications using test-particle methods [26,27]. As the basic feature of these approaches the energy and momentum of the test particles are no longer related by the mass-shell condition but according to their spectral distributions. Thus particles are propagated and also scattered off mass shell. Hence, knowledge of off-shell scattering amplitudes becomes necessary. However, the behavior of such amplitudes is presently unknown to a large extent. The off-shell structure of the scattering amplitude determines in this context also the magnitude of nonlocal corrections to the Boltzmann equation which can be translated into nonlocal time and momentum shifts in the binary scattering process [28].

Here again the relativistic Brueckner approach provides a natural tool to determine in-medium off-shell scattering amplitudes in the ladder approximation. In the present work we extend the on-shell *NN* scattering to the half-off-shell case where the incoming particles are still on their mass shells but the final states are generally off shell. These matrix elements provide valuable information for future transport investigations beyond the QPA. We investigate the off-shell structure of the in-medium *T* matrix—respectively, the transition amplitudes $|T|^2$ and the resulting cross sections—over a wide range of nuclear matter densities.

The paper is organized as follows. First (Sec. II) we briefly sketch the basic features of the relativistic Brueckner approach. In Sec. III the on-shell scattering problem in the medium is discussed. Neutron-neutron and proton-proton channels are considered separately, and total and differential cross section are given. We also compare with the results of other groups, mainly those of Li and Machleidt [21]. In Sec. IV we turn to the half-off-shell case and discuss the structure of transition amplitudes and cross sections beyond the quasiparticle approximation and summarize in Sec. V.

II. RELATIVISTIC BRUECKNER APPROACH

In the relativistic Brueckner approach the Bethe-Salpeter equation is reduced to a three-dimensional integral equation of the Lippmann-Schwinger type, the so-called Thompson equation [29]. The Thompson propagator projects thereby the intermediate nucleons onto positive-energy states and restricts the exchanged energy transfer by $\delta(k^0)$ to zero. The Thompson equation is most easily solved in the two-nucleon c.m. frame:

$$T(\mathbf{p},\mathbf{q},\mathbf{P})|_{\mathrm{c.m.}} = V(\mathbf{p},\mathbf{q}) + \int \frac{d^3\mathbf{k}}{(2\pi)^3} V(\mathbf{p},\mathbf{k}) \times \frac{M^{*2}}{E^{*2}(\mathbf{k})} \frac{Q(\mathbf{k},\mathbf{P})}{2E^*(\mathbf{q}) - 2E^*(\mathbf{k}) + i\epsilon} T(\mathbf{k},\mathbf{q},\mathbf{P}), \tag{1}$$

where $\mathbf{q} = (\mathbf{q}_1 - \mathbf{q}_2)/2 = (\mathbf{q}_1^* - \mathbf{q}_2^*)/2$ is the relative momentum of the initial states and similar **p,k** are the relative momenta of the final and intermediate states, respectively. $\mathbf{P} = (\mathbf{q}_1 + \mathbf{q}_2)$ is the c.m. momentum. The starting energy in Eq. (1) is fixed to $\sqrt{s^*} = 2E^*(\mathbf{q})$. Sandwiching the one-boson-exchange potential *V*, Eq. (1), between in-medium spinors, Eq. (4), the matrix elements acquire a density dependence which is absent in nonrelativistic treatments and which is believed to be the major reason for the much improved description of the nuclear saturation properties [3] in the relativistic theory. The Pauli operator *Q* prevents intermediate states from scattering into forbidden phase space areas.

Inside the medium the particles are dressed which leads to effective masses and the kinetic momentum:

$$M^*(k) = M + \mathrm{Re}\Sigma_s(k), \quad k^{*\mu} = k^\mu + \mathrm{Re}\Sigma^\mu(k). \tag{2}$$

Re and Im denote the real and imaginary parts since (above the Fermi surface) the self-energy is generally complex. Here we adopt the *quasiparticle approximation*; i.e., the Im [Σ] will be neglected in Eq. (1). This means that the decay width of the dressed nucleon state *k* to another state *k'* is set equal to zero, resulting in an infinite lifetime of this ''quasiparticle'' state. Furthermore, the explicit momentum dependence of the self-energy which enters via a term $\mathbf{k}\Sigma_v$ proportional to the spatial component Σ_v of the vector self-energy is small and can be dealt with by introducing the reduced kinetic momentum $\tilde{k}^{*\mu} = k^{*\mu}/(1+\Sigma_v)$ and the reduced effective mass $\tilde{M}^* = M^*/(1+\Sigma_v)$ [7]. Thus, the nucleons are given by plane waves which fulfill a quasifree Dirac equation

$$[\gamma_\mu \tilde{k}^{*\mu} - \tilde{M}^*] u_\lambda(k) = 0. \tag{3}$$

Using the normalization of Ref. [8] the self-consistent positive-energy spinors of helicity λ are defined as

$$u_\lambda(k) = \sqrt{\frac{\tilde{E}^*(k) + \tilde{M}^*}{2\tilde{M}^*}} \begin{pmatrix} 1 \\ \dfrac{2\lambda|\mathbf{k}|}{\tilde{E}^*(k) + \tilde{M}^*} \end{pmatrix} \chi_\lambda, \tag{4}$$

with χ_λ being a Pauli spinor. The Dirac spinors depend on the effective mass and thus on the nuclear density. In the

Thompson equation (1) and in the discussion below we deal with the rescaled quantities $\tilde{M}^*$ and $\tilde{k}^*$ but will omit this in the notation further on.

To summarize the kinematics of the Thompson equation (i) the initial states are on shell, i.e., $q_\mu=\{E^*(\mathbf{q}),\pm\mathbf{q}\}$ with $E^*(\mathbf{q})=\sqrt{M^{*2}+\mathbf{q}^2}=\frac{1}{2}\sqrt{s^*}$. The final states fulfil energy-momentum conservation $p_\mu=\{\frac{1}{2}\sqrt{s^*},\pm\mathbf{p}\}$ and are off shell as soon as $|\mathbf{p}|\neq|\mathbf{q}|$. (ii) The determination of the off-shell matrix elements is perturbative in the sense that the quasiparticle approximation is applied to the Thompson equation, although T is generally complex for incident momenta above the Fermi surface which leads to a nonvanishing imaginary part of the self-energy $\mathrm{Im}\,\Sigma$ and, correspondingly, an imaginary optical potential [8,11].

To determine the scalar Σ_s and vector components Σ_0 and Σ_v of the self-energy is a subtle problem. Here on-shell ambiguities arise from the projection onto positive-energy states when the T matrix is decomposed into Lorentz invariant amplitudes. This problem has been known for a long time [8,9] and is still not completely resolved. In [12] we discussed the failure of previously used recipes [8,11] which led to spurious contributions in the self-energy from the coupling to negative-energy states, in particular spurious contributions from a pseudoscalar one-pion exchange which are not completely replaced by a pseudovector coupling. In Ref. [13] this problem was extensively discussed and a method to minimize the on-shell ambiguities was proposed. Here we used the scheme of [13] where the Born term V and the remaining ladder kernel of the Thompson equation are treated separately. Thus we account properly for the pseudovector structure of the Born contributions $V_{\pi,\eta}$ from π- and η-exchange contributions when the projection of the full T matrix onto covariant amplitudes is performed. The remaining ladder kernel thereby is treated as a pseudoscalar.

To solve the Thompson equation (1) in the c.m. system we apply standard techniques which are in detail described by Erkelenz [30]. After a partial-wave projection onto the $|JMLS\rangle$ states the integral reduces to a one-dimensional integral over the relative momentum $|\mathbf{k}|$ and Eq. (1) decouples into three subsystems of integral equations for the uncoupled spin singlet, the uncoupled spin triplet, and the coupled triplet states. As a result of the antisymmetry of the two-fermion states, we can restore the total isospin ($I=0,1$) of the two-nucleon system with the help of the selection rule $(-)^{L+S+\mathrm{I}}=-1$ which means that matrix elements are already antisymmetrized.

The Pauli operator Q is replaced by an angle-averaged Pauli operator $\overline{Q}$. For nonvanishing c.m. momenta the Fermi sphere is in the two-nucleon c.m. frame deformed to a Fermi ellipsoid for which $\overline{Q}$ has to be evaluated [7,8]. We are solving the integral equations by the matrix inversion techniques of Haftel and Tabakin [31]. Real and imaginary parts of the T matrix are calculated separately by the principal-value treatment given by Trefz *et al.* [32]. From there it is seen that $\mathrm{Im}\,T$ is essentially proportional to the angle-averaged Pauli operator and thus it is strongly reduced for momenta below the Fermi surface due to Pauli blocking. Then positive-energy helicity T-matrix elements are constructed from the $|JMLS\rangle$ scheme as described in [10,30]. From general symmetries it follows that for each total angular momentum J only six of the 16 helicity matrix elements are independent:

$$T_1=\langle++|T^J(p,q)|++\rangle,\quad T_2=\langle++|T^J(p,q)|--\rangle,$$
$$T_3=\langle+-|T^J(p,q)|+-\rangle,\quad T_4=\langle+-|T^J(p,q)|-+\rangle,$$
$$T_5=\langle++|T^J(p,q)|+-\rangle,\quad T_6=\langle+-|T^J(p,q)|++\rangle, \tag{5}$$

which in the on-shell case $|\mathbf{p}|=|\mathbf{q}|$ further reduce to five independent matrix elements since then $T_5=T_6$. From the six independent amplitudes in the $|JMLS\rangle$ representation the six independent partial-wave amplitudes (5) in the helicity representation (for $I=0,1$ and real and imaginary parts separately) are obtained as described in Ref. [30]. Summation over J yields the full helicity matrix elements (5):

$$\sum_J\left[\frac{2J+1}{4\pi}\right]d^J_{\lambda\lambda'}(\theta)\langle\lambda_1'\lambda_2'|T^J(p,q)|\lambda_1\lambda_2\rangle$$
$$=\langle\mathbf{p}\lambda_1'\lambda_2'|\hat{T}|\mathbf{q}\lambda_1\lambda_2\rangle. \tag{6}$$

Here θ is the scattering angle between $\mathbf{q}$ and $\mathbf{p}$ and $\lambda=\lambda_1-\lambda_2,\lambda'=\lambda_1'-\lambda_2'$. The reduced rotation matrices $d^J_{\lambda\lambda'}(\theta)$ are those defined by Rose [33]. The matrix elements on the left hand side of Eq. (6) are independent of the third component of the isospin I_3 and depend only on the absolute values p,q of the momenta.

III. ON-SHELL SCATTERING

The on-shell nucleon-nucleon cross section can be directly determined from the T-matrix amplitudes. In this case the extension to off-shell scattering is straightforward. Another possibility is to determine the on-shell phase shifts [21,30]. Doing so, an extension to the off-shell case is, however, unclear. Furthermore, the definition of the vacuum phase shifts (see, e.g., Refs. [10,30]) has to be modified inside the medium to account for the modified unitarity relations. To be more precise, the definition of in-medium phase shifts should include the Pauli operator as pointed out in [16,17]. To avoid such problems we will directly determine the cross sections from the matrix elements. The squared matrix elements are given as

$$|\hat{T}(p,q,\theta)|^2=\sum_{i=1}^{6}\beta_i\left[\left(\sum_J\frac{2J+1}{4\pi}d^J_{\lambda_i\lambda_i'}(\theta)\,\mathrm{Re}\,T_i^J(p,q)\right)^2\right.$$
$$\left.+\left(\sum_J\frac{2J+1}{4\pi}d^J_{\lambda_i\lambda_i'}(\theta)\,\mathrm{Im}\,T_i^J(p,q)\right)^2\right]. \tag{7}$$

The weighting factors $\beta_i=2$, $i=1,\ldots,4$, and $\beta_5=\beta_6=4$ arise from the sum over all helicity states. Using the orthogonality relation for the rotation matrices,

$$\int d\cos(\theta)d^J_{\lambda\lambda'}(\theta)d^{J'}_{\lambda\lambda'}(\theta)=\frac{2}{2J+1}\delta_{JJ'}, \tag{8}$$

one obtains

$$\int d\Omega |\hat{T}(p,q,\theta)|^2 = \sum_{i=1}^{6} \beta_i \sum_J \frac{2J+1}{4\pi} \{[\mathrm{Re}\, T_i^J(p,q)]^2 + [\mathrm{Im}\, T_i^J(p,q)]^2\}. \quad (9)$$

In the on-shell case $p=q$ the differential cross section follows from the matrix elements by the standard expression

$$d\sigma = \frac{(M^*)^4}{s^* 4\pi^2} |\hat{T}(q,q,\theta)|^2 d\Omega. \quad (10)$$

A. Free cross section

The predictions of the Bonn potentials for free NN cross sections have in detail been discussed by Li and Machleidt [21]. Throughout this work we apply the Bonn A potential [14] and the results of [21] for the vacuum case are reproduced with high accuracy for both differential and total cross sections. To demonstrate this feature, the results from [21] are included in Figs. 6 and 7 where the total neutron-proton $[T_i^J = 0.5(T_i^{J,I=0} + T_i^{J,I=1})]$ and proton-proton $(T_i^J = T_i^{J,I=1})$ cross sections are shown. As found in [21] the pp cross section is in particular at low energies significantly smaller than the np cross section. It should, however, be noted that in the present work as well as in Ref. [21] the pp cross sections are not Coulomb corrected.

B. In-medium cross section

As already pointed out in Refs. [18,19] a trivial medium modification of the cross sections arises from the in-medium masses entering into the kinematical term $(M^*)^4/s^*$ in Eq. (10) which is due to the normalization of the relativistic spinor basis and the incoming flux. This phase space factor reduces the in-medium cross section by the order of $(M^*/M)^2$ at small momenta.

Besides the fact that one deals with dressed quasiparticles the essential feature of the Bethe-Goldstone or Bethe-Salpeter equation, respectively, is the occurrence of the Pauli operator. This means that the vacuum relations which connect the phase shifts with the real reaction matrix R are modified by the Pauli operator. In a schematic notation[1] the in-medium reaction matrix R is connected to the T matrix by [10,32]

$$\hat{R} - \hat{T} = i\pi \hat{R} Q \hat{T}, \quad (11)$$

which leads to a modified optical theorem

$$|\hat{T}|^2 = \frac{\hat{R}^2}{1+(\pi \hat{R} Q)^2} = (\pi Q)^{-1} |\mathrm{Im}\, \hat{T}|. \quad (12)$$

[1]For clarity of notation we suppress in Eqs. (11)–(13) factors M^*/E^* which can be absorbed into R and T [10] and the δ function originating from the principal-value treatment of the Blankenbecler-Sugar and Thompson propagators, respectively.

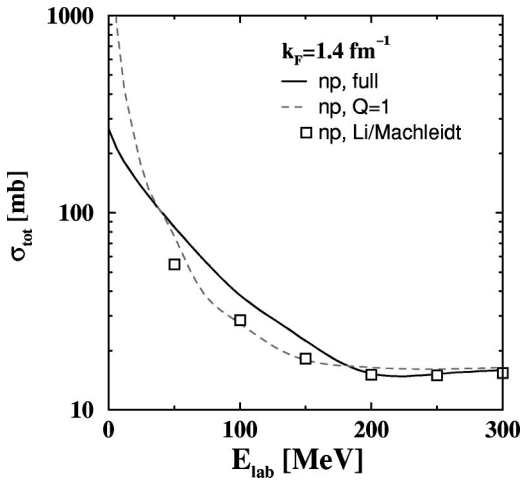

FIG. 1. Total np in-medium cross section at $k_F = 1.4$ fm^{-1}. The result of the full calculation is compared to a calculation where the Pauli operator in the Thompson equation for the intermediate scattering states has been switched off $(Q=1)$. Also the corresponding result of Ref. [21] is shown.

With $Q=1$ the vacuum expressions are recovered. The modification of the optical theorem by the presence of the medium, in particular the appearance of the inverse Pauli operator which compensates at momenta below the Fermi surface for the vanishing $\mathrm{Im}\, \hat{T}$, has been discussed in [16,17,32]. It becomes clear from Eq. (12) that the use of the vacuum relations (with $Q=1$) to extract phase shifts from the in-medium reaction matrix R is an approximation justified at low densities and/or high energies. In between the Pauli operator is essentially different from unity and appears in the denominator of Eq. (12). Neglecting here the influence of the Pauli operator will lead to an underestimation of the corresponding cross sections. The real and imaginary parts of the T matrix are related to the reaction matrix by [32]

$$\mathrm{Re}\, \hat{T} = \frac{\hat{R}}{1+(\pi \hat{R} Q)^2}, \quad \mathrm{Im}\, \hat{T} = -\frac{\pi Q \hat{R}^2}{1+(\pi \hat{R} Q)^2}. \quad (13)$$

We emphasise this point because, as will be seen in the following, we find the in-medium cross sections to be substantially less suppressed at low momenta than found by Li and Machleidt [21] whereas we obtain good agreement with their results at high momenta. The reason for the deviations can be traced back to the different procedures used to determine the cross sections. As discussed in Sec. II the squared matrix elements (7) provide an unambiguous and direct method to extract the cross section. To determine phase shifts first has to be done with caution since the occurrence of the Pauli operator modifies the corresponding phase shift relations in the medium [16]. If neglected, as done in the approximation used in Ref. [21], this effect leads in particular at low momenta to an underprediction of the cross section. To illustrate this effect in Fig. 4 we investigate the influence of the Pauli operator on the in-medium np cross section. For a fair comparison the density $(k_F = 1.4$ fm$^{-1})$ as well as the value of M^* is chosen as in Ref. [21]. One curve in Fig. 1 is obtained

by switching off the Pauli operator in the Thompson equation (1), i.e., setting $\overline{Q}\equiv 1$. It is clearly seen that the influence of the Pauli operator leads even to an enhancement of the cross section at momenta below $\simeq 180$ MeV compared to the $\overline{Q}\equiv 1$ case which is due to the occurrence of Q in the denominator in Eqs. (12) and (13). As expected, at very small momenta the presence of the Pauli operator leads to a significant suppression of the cross section. One should, however, keep in mind that the Pauli operator acts here only on the *intermediate* states in the Thompson equation (1) and not on the final states. Thus full Pauli blocking $\overline{Q}\equiv 0$ reduces the full T matrix to its Born part $\hat{V}$. In the transport approach, on the other hand, the Pauli blocking prevents also the scattering into occupied final states. Thus Fig. 4 refers only to Pauli effects in the intermediate states, but demonstrates the importance of accounting properly for the Pauli operator in the in-medium optical theorem (12).

In the following we consider the in-medium cross sections at four different Fermi momenta $k_F = 1.1$, 1.34, 1.7, and 1.9 MeV, which corresponds to densities $\rho = 0.090$, 0.1625, 0.332, and 0.4633 fm^{-3}. For simplicity we denote these densities in the text as $0.5\rho_0$, ρ_0, $2\rho_0$, and $3\rho_0$ although these values do not exactly correspond to multiples of $\rho_0 = 0.1625$ fm^{-3}. Again all calculations are performed using the Bonn A potential. The in-medium mass M^* entering into Eq. (10) has in our calculation the values $M^* = 766.6$, 646.7, 433.6, and 310.1 MeV. These values are slightly larger than those of Refs. [21,10]. Thus we expect also slightly larger values for the in-medium cross section, in particular at low momenta, which are due to higher values of the kinematical factor $(M^*)^4/s^*$. The reason for the different effective masses lies in different solution techniques for the Thompson equation (1). As discussed in Sec. II, we apply a refined projection scheme in order to transform the T matrix from the two-particle c.m. frame to the nuclear matter rest frame where the self-energy components (2) are determined [12,13]. In the medium the on-shell T matrix (1) depends on three variables: the relative momentum $\mathbf{q}$ of the initial states, the scattering angle θ, and the center-of-mass momentum $\mathbf{P}$ of the two-particle c.m. frame relative to the nuclear matter rest frame. As in Refs. [21,16,17] we consider only the case where the two-particle c.m. frame and the nuclear matter rest frame coincide, i.e., $\mathbf{P}=0$.

In Fig. 2 the differential np cross section at the different densities is shown at fixed relative momentum $|\mathbf{q}| = 342$ MeV which in the vacuum corresponds to a laboratory energy of $E_{\rm lab} = 2\mathbf{q}^2/M = 250$ MeV. The vacuum definition of $E_{\rm lab}$ was used in [21] to compare the cross sections at different densities. The presence of the medium tends to make the np differential cross section more isotropic. At backward angles the cross sections are decreasing with density. At forward angles the behavior is more complicated: At moderate densities ($\rho = 0.5\rho_0$ and $1\rho_0$) the cross section is reduced but at high densities ($\rho = 2\rho_0$ and $3\rho_0$) a strong enhancement of the forward scattering amplitude can be observed. It is worth noticing that in this energy range we are in good agreement with the results obtained by Li and Machleidt [21]. Similar results have been obtained at $0.5\rho_0$, ρ_0, and $2\rho_0$, and also at $2\rho_0$ the cross section was found to be enhanced at forward angles compared to ρ_0. Going higher in density ($3\rho_0$) we find this effect even more pronounced. While the cross section stays now almost constant at backward angles, it is strongly enhanced at forward angles. However, at $3\rho_0$ the cross section is highly anisotropic and dominated by a p-wave component. Here we see a suppression of higher partial waves with increasing density. At $3\rho_0$ one needs partial waves up to at least $J \leqslant 6$ to approximate the full result ($J = 12$), at $2\rho_0$ the partial waves $J \leqslant 4$ are almost sufficient, and at $3\rho_0$ the behavior is like an $s+p$ wave with $J \leqslant 1$. Figure 3 shows the same for pp scattering. Again our results are in good agreement with the findings of Ref. [21]. In the $I=1$ channel (pp) the cross sections are generally more isotropic than in the np channel. With rising density

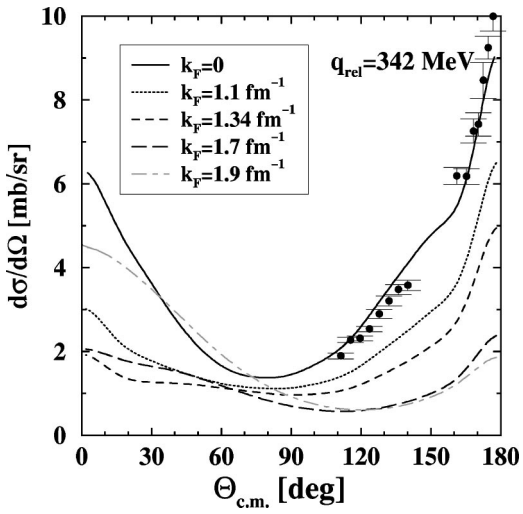

FIG. 2. Differential np in-medium cross section at fixed relative c.m. momentum $|\mathbf{q}| = 342$ MeV ($2\mathbf{q}^2/M = 250$ MeV) at various densities. Experimental data from [34] for the free scattering are included.

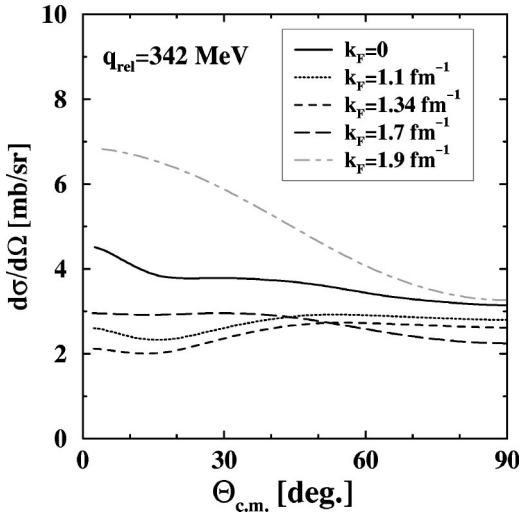

FIG. 3. Differential pp in-medium cross section at fixed relative c.m. momentum $|\mathbf{q}| = 342$ MeV ($2\mathbf{q}^2/M = 250$ MeV) at various densities.

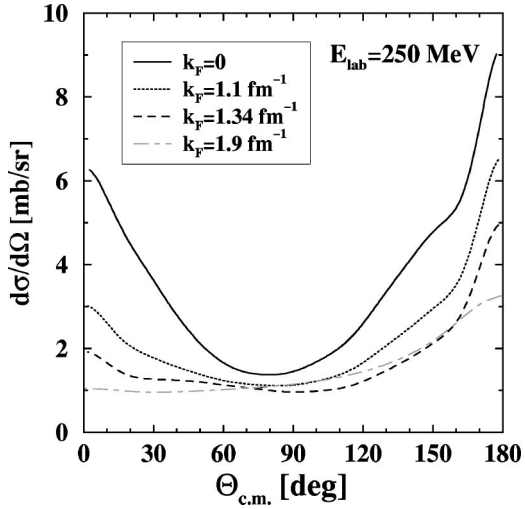

FIG. 4. Differential np in-medium cross section at laboratory energy $E_{\mathrm{lab}}(\rho)\simeq 250$ MeV at various densities.

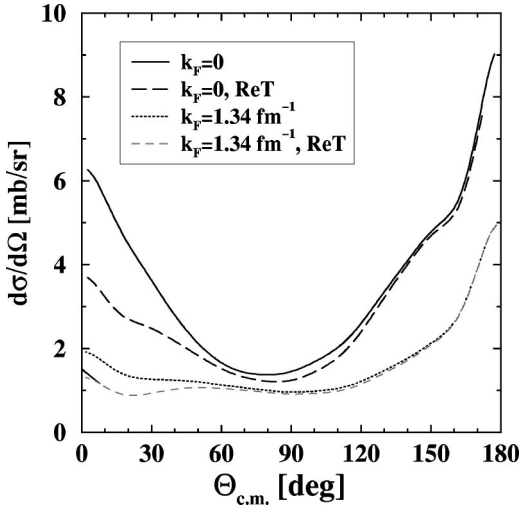

FIG. 5. Differential np in-medium cross section at fixed relative c.m. momentum $|\mathbf{q}|=342$ MeV in the vacuum (upper curves) and at $k_F=1.34$ (ρ_0) (lower curves). The contributions from the real part of the T matrix are shown separately.

the cross sections are first decreasing ($0.5\rho_0$, ρ_0) and then increasing. At $3\rho_0$ we observe a dramatic increase of the cross section at forward angles. In the pp cross section the contributions of higher partial waves are reduced with growing density; e.g., at ρ_0 partial waves up to $J\leqslant 4$ reproduced the full result quite well whereas at $3\rho_0$ only contributions from $J\leqslant 3$ are relevant.

The peculiar behavior at $3\rho_0$ seen in Figs. 2 and 3 can be understood from the presence of the mean field. In Figs. 2 and 3 we investigated the density dependence of the cross sections at an equivalent relative c.m. momentum $\mathbf{q}$. This does, however, not correspond to equivalent energies. At finite density the laboratory energy $E_{\mathrm{lab}}(|\mathbf{q}|,\rho)=E(|\mathbf{q}|,\rho)-M$ is given by

$$E_{\mathrm{lab}}=\frac{2\mathbf{q}^2}{M^*}+\Sigma_s-\Sigma_0 \tag{14}$$

and is therefore strongly modified by the presence of the mean field. At high densities the energy scale is stretched by the decreasing effective mass M^*. This effect is responsible for the suppression of higher partial-wave contributions to the differential cross section above $2\rho_0$ if one compares the cross sections at identical c.m. momenta but at essentially different incident energies.

To illustrate this effect in Fig. 4 we show the density dependence of the differential np cross section at the same laboratory energy $E_{\mathrm{lab}}\simeq 250$ MeV. At comparable energies rather than comparable c.m. momenta the difference in the differential cross section at ρ_0 and $3\rho_0$ is now much less pronounced.

The suppression of the in-medium cross section at forward angles which occurs at higher densities can be understood from Fig. 5 and Eq. (13). This figure illustrates the influence of the Pauli operator and the imaginary part of the T matrix. It is seen that at ρ_0 the imaginary part of T which contributes in the vacuum by about 50% to the forward scattering amplitude ($\theta=0$) is now strongly suppressed by the Pauli operator. This effects is maximal at low momenta and high densities. When $\mathbf{q}$ lies below the Fermi surface the imaginary part of T vanishes completely. Thus, Pauli blocking in the intermediate states makes the cross section more isotropic.

In Figs. 6 and 7 we show the total in-medium np and pp cross sections in the considered density range $0.5\rho_0$–$3\rho_0$ as a function of E_{lab}, Eq. (14). Using this quantity the scale is considerably stretched compared to the vacuum expression $2\mathbf{q}^2/M$ (used in [21]). There are two major aspects to be noticed: At high energies $E_{\mathrm{lab}}\geqslant 200$ MeV we find good agreement with the previous calculations of Ref. [21]. For np as well as pp scattering the cross sections reach asymptotic values around 15–20 mb. At high densities the cross section has the tendency to rise again with increasing laboratory energy. This behavior is even more pronounced in

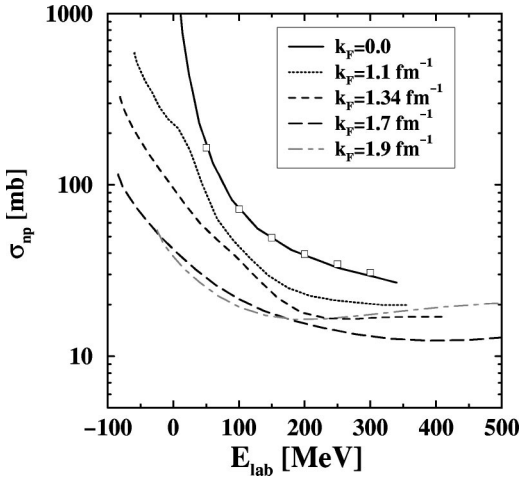

FIG. 6. Total np in-medium cross section at various densities as a function of $E_{\mathrm{lab}}(\rho)$. In addition the results of [21] (squares) for the free cross section are shown.

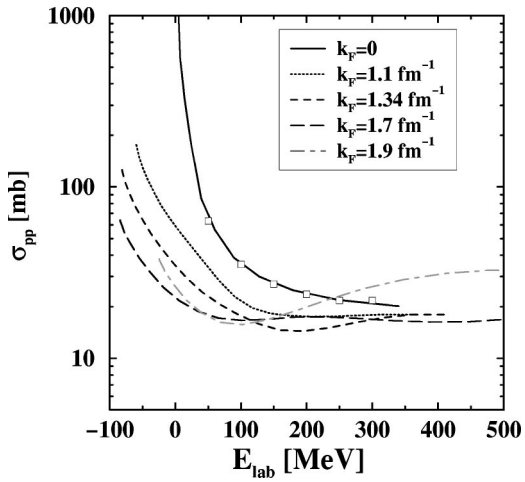

FIG. 7. Total pp in-medium cross section at various densities as a function of $E_{\rm lab}(\rho)$. In addition the results of [21] (squares) for the free cross section are shown.

the proton-proton channel and has been observed by other groups as well [18,21].

At low energies the in-medium cross sections are considerably less suppressed than observed in Ref. [21]. One reason is our somewhat larger values for the in-medium mass, but this effect is not sufficient to explain the deviations at low energies. As illustrated by Fig. 1 the differences can be understood by the low-density and high-momentum approximation made in [21] which neglects the influence of the Pauli operator in the optical theorem. Besides this point, at $0.5\rho_0$ we see a small additional enhancement of the np cross section around an energy of 15 MeV which is not present in the pp channel. A much stronger enhancement of the cross section at low densities has been observed by Alm *et al.* [17]. In the finite temperature approach of [17] this critical enhancement is attributed to the onset of superfluidity. Crucial for such a superfluid state are contributions from hole-hole scattering in the Pauli operator which are absent in the standard Brueckner approach (used here). However, as discussed in [35] a signature of a bound pair state can appear at low densities even when hole-hole scattering is neglected in the Pauli operator. In the present calculations such a resonance-like enhancement of the cross section is only seen in the $I=0$ amplitudes which correspond to the quantum numbers of the deuteron, i.e., the $^3S_1$, $^3D_1$, and the $^3S_1$-$^3D_1$ transition channels. Therefore the low-density enhancement of the np cross section can be interpreted as a precursor of a superfluid state and supports the findings of [35].

IV. HALF OFF-SHELL SCATTERING

A. Matrix elements

In the following we consider the case of half-off-shell scattering. This means that the initial states with c.m. momenta $\pm\mathbf{q}$ are on their mass shell $E^*(\mathbf{q})=\sqrt{\mathbf{q}^2+M^{*2}}$. However, now the momenta of the final states $\pm\mathbf{p}$ can vary independently, i.e., $|\mathbf{p}|\neq|\mathbf{q}|$. Since the requirement of energy conservation fixes the final energies $p_\mu=\{p_0,\pm\mathbf{p}\}$ to $p_0=\frac{1}{2}\sqrt{s^*}=E^*(\mathbf{q})$, these states are off energy shell. To obtain an impression as to how the off-shellness affects the T-matrix amplitudes we consider first the matrix elements. In the on-shell case the cross sections follow from the squared matrix elements $|T(q,q)|^2$ by Eq. (10). The squared matrix elements $|T(p,q)|^2=\int|T(p,q,\theta)|^2d\Omega$ are also those quantities which enter directly into a generalized transport equation as transition amplitudes for off-shell scattering [27]. In that case it makes more sense to speak in terms of transition amplitudes than in terms of cross sections. The latter are obtained from the transition amplitudes by integration over the final state spectral distributions. Thus, the cross sections depend crucially on the spectral width of the particles whereas the transition amplitudes themselves are independent of the spectral functions.

In Fig. 8 we show the isospin-averaged matrix elements $|T(p,q)|^2$ for NN scattering as a function of p and q at nuclear matter densities $0.5\rho_0$, ρ_0, $2\rho_0$, and $3\rho_0$. The amplitudes $|T|^2$ are given in fm^4 and have to be multiplied by the factor $(2\pi)^6$ (due to our normalization of the T matrix) when they are inserted into Eq. (10) to obtain cross sections. The diagonal $(p=q)$ on-shell elements correspond to the total cross section. First of all, it is seen that the amplitudes $|T|^2$ show the same behavior as the corresponding (on-shell) cross sections, namely, a general decrease with momentum and density. In the cross section this tendency is just enhanced by the kinematical factor M^{*4}/s^* which decreases with density and also with momentum.

The off-shellness of the final states now given by

$$\Delta\omega=E^*(\mathbf{q})-E^*(\mathbf{p})\simeq\frac{\mathbf{q}^2-\mathbf{p}^2}{2M^*}, \tag{15}$$

which is maximal perpendicular to the diagonal. It can be seen from Fig. 8 that at low momenta the matrix elements are only weakly affected by the fact that the outgoing states are off energy shell. This does not mean that the matrix elements do not change going away from the on-shell point. Indeed, the variation of the matrix elements is considerable as will become even more clear further on. However, the dependence of the matrix elements is nearly symmetric in q and p, i.e.,

$$|T(p,q)|^2\simeq|T(q,p)|^2, \tag{16}$$

and thus not strongly affected by the off-shellness of the outgoing states. In particular in the low-momentum region the matrix elements fall off symmetrically with increasing momenta p and/or q. Only at the highest density of $3\rho_0$ is the asymmetry rather pronounced. The off-shell variation of the outgoing states leads here to a resonance structure around $q=250$ MeV where the amplitudes increase with different strengths in p and q directions. The off-shell behavior is similar in the np and pp channels, except that the resonance structure at $3\rho_0$ is more pronounced in the latter case. The somewhat stronger off-shell dependence of the pp scattering at high densities is also reflected in the stronger reduction of the corresponding total cross section shown in Figs. 11 and 12.

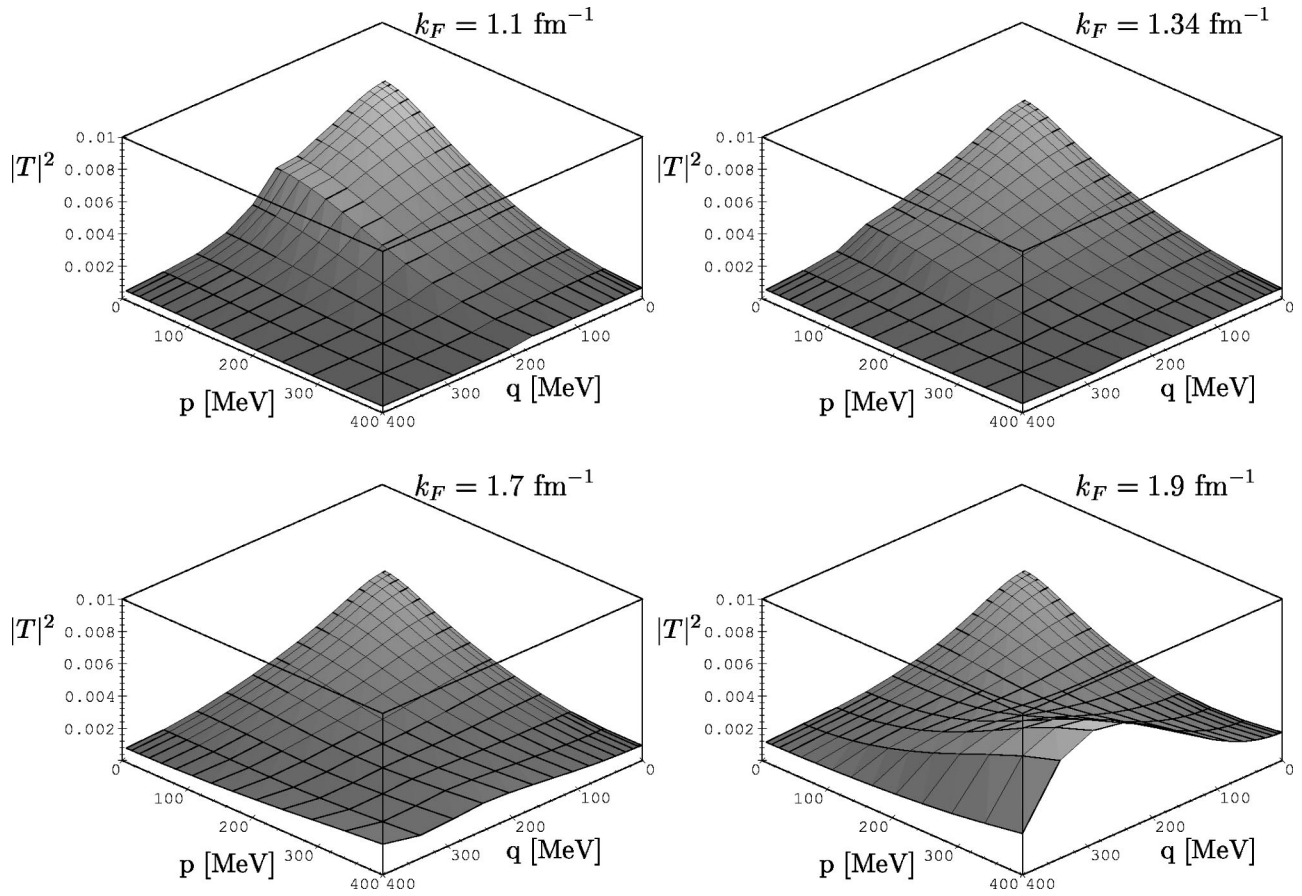

FIG. 8. Squared isospin averaged half-off-shell T-matrix elements $|T|^2$ in [fm^4] at various densities. The initial states with relative c.m. momentum q are on shell, and the final states with relative c.m. momentum p are off shell.

In order to obtain a more quantitative impression of the off-shell dependence next we investigate the deviation of the amplitudes $\delta|T|^2$ from their on-shell values as a function of the off-shellness $\delta\omega$ of the final states. $\delta|T|^2$ is thereby defined as the relative deviation, i.e.,

$$\delta|T|^2 = \frac{|T(q,\delta\omega)|^2 - |T(q,\delta\omega=0)|^2}{|T(q,\delta\omega=0)|^2}. \tag{17}$$

For a better comparison of the different densities the variable $\delta\omega$, i.e., the energy shift of the final states with momenta $\pm\mathbf{p}$ relative to their on-shell energies, is scaled by the effective mass:

$$\delta\omega = \frac{M^*}{M}[E^*(\mathbf{q}) - E^*(\mathbf{p})]. \tag{18}$$

The range for the variation of $\delta\omega$ is constrained by the kinematical limits of our calculations, i.e., $0 \leqslant p,q \leqslant 400$ MeV. The symmetric falloff with p and q in the low-momentum range which is reflected in Fig. 8 implies already the following tendency: For $p<q$, i.e., $\delta\omega>0$, one expects an enhancement of the amplitudes, i.e., $\delta|T|^2>0$, whereas for $p>q$, i.e., $\delta\omega<0$, one expects a reduction of the amplitudes. For small values of q this behavior is clearly seen from Fig. 9. There the deviation of the isospin-averaged matrix elements $\delta|T|^2$ from the on-shell point is shown at fixed values of the on-shell momentum $q=100$, 200, 300, and 400 MeV. First of all we see that the variation of the amplitudes is pronounced. Within the range of $\delta\omega=\pm 50$ MeV the matrix elements can easily vary by more than $\pm 100\%$. Second, we find that the patterns are similar at moderate densities $0.5\rho_0$ and ρ_0 but become essentially different at large densities $\rho \geqslant 2\rho_0$. Thus, the off-shell behavior reflects a strong medium dependence. The systematics of the different pattern is, however, quite complex.

Let us first consider moderate nuclear matter densities. At low momenta q the amplitudes show an extremely strong variation around the on-shell point which reflects their steep and symmetric fall off (see Fig. 8). As already mentioned, this results in a strong suppression at negative $\delta\omega$ and an equally strong enhancement at positive $\delta\omega$. In the high-momentum region the variation of the amplitudes is much weaker which results in a smoother and less pronounced dependence on $\delta\omega$. With increasing density the situation changes drastically and is even reversed at large q: now the amplitudes are strongly enhanced in the negative-$\delta\omega$ region and reduced at positive $\delta\omega$. This reflects the asymmetry of $|T|^2$ around the on-shell diagonal seen in Fig. 8 in the high-momentum range.

To summarize, the half-off-shell matrix elements show a pronounced density dependence. At moderate densities, how-

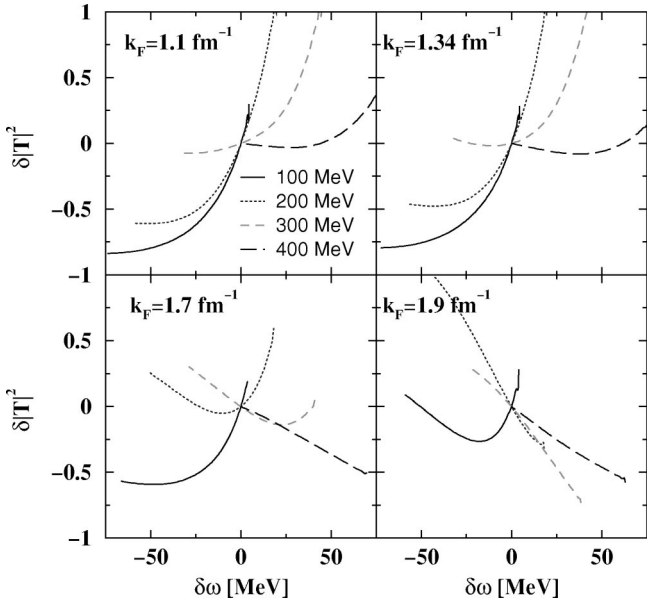

FIG. 9. Relative deviation of the isospin-averaged T-matrix elements $|T|^2$ from their values at the on-shell point as a function of the off-shellness $\delta\omega$ of the final states. $\delta|T|^2$ is shown for various densities at fixed incoming relative momenta $q=100$, 200, 300, and 400 MeV.

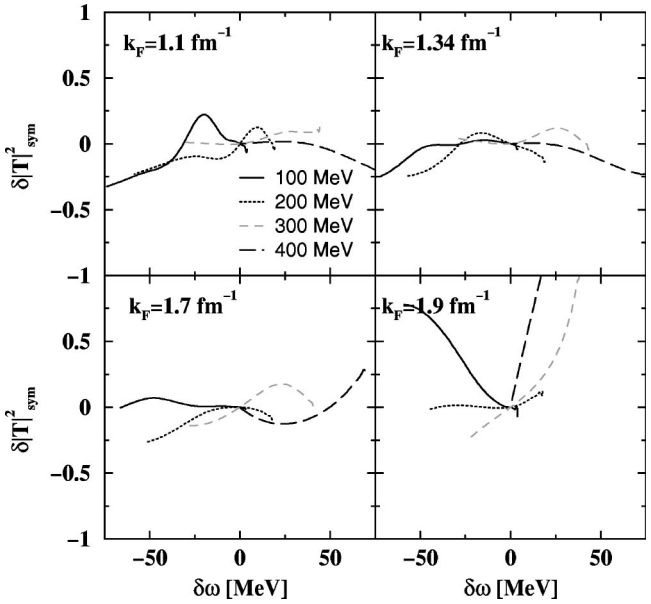

FIG. 10. Relative deviation of the isospin-averaged approximated T-matrix elements $|T|^2$, Eq. (19), from their exact off-shell values as a function of the off-shellness $\delta\omega$ of the final states. $\delta|T|^2$ is shown for various densities at fixed incoming relative momenta of $q=100$, 200, 300, and 400 MeV.

ever, the dependence on the incident on-shell momenta q and the final momenta p which are off shell is to a large extent symmetric in p and q. This implies that the matrix elements are not too much affected by the shift to off-shell energies but are mainly determined by the absolute values of the momentum states p and q. As a consequence, the off-shell matrix elements can be approximated with an accuracy of about 10–30 % by the on-shell points in the following way:

$$|T(p,q)|^2 \simeq |T(\bar{q},\bar{q})|^2, \quad \bar{q}=\sqrt{\frac{1}{2}(p^2+q^2)}, \tag{19}$$

which follows from the symmetry assumption (16). At large nuclear matter densities this symmetry is more strongly violated, i.e., by about 20–40 % at $2\rho_0$. Nevertheless, in view of the extremely large variation of the matrix elements with $\delta\omega$, ranging from almost complete suppression to an enhancement of more than a factor of 2, the accuracy of this symmetry assumption is quite good in the considered $\delta\omega$ interval. It can be applied in a straightforward way, e.g., in transport calculations, and requires only knowledge of the on-shell matrix elements. However, at $3\rho_0$ the amplitudes are highly asymmetric in p and q and thus approximation (19) does no longer hold. Here an accurate description requires knowledge of the exact matrix elements.

Figure 10 illustrates the validity of the symmetry assumption (19) and the strength of the explicit dependence of the matrix elements on the energy shift $\delta\omega$. There the relative deviations

$$\delta|T|^2_{\rm sym}=\frac{|T(\bar{q},\bar{q})|^2-|T(p,q)|^2}{|T(p,q)|^2} \tag{20}$$

from the exact results $|T(p,q)|^2$ are shown as functions of $\delta\omega$, again for fixed values of q.

B. Cross sections

A cross section is obtained from the transition amplitudes $|T|^2$ by division through the incoming flux,

$$v_{12}=\frac{F^*(q_1,q_2)}{E^*(\mathbf{q}_1)E^*(\mathbf{q}_2)}=\frac{\sqrt{(q_1\cdot q_2)^2-M^{*4}}}{E^*(\mathbf{q}_1)E^*(\mathbf{q}_2)}, \tag{21}$$

and multiplication by the final state phase space factors,

$$d\sigma=\frac{M^{*4}}{F^*}(2\pi)^4\delta^4(q_1+q_2-p_1-p_2)$$
$$\times|T(p_1p_2,q_1q_2)|^2\frac{d^4p_1}{(2\pi)^4}A(p_1)\frac{d^4p_2}{(2\pi)^4}A(p_2). \tag{22}$$

The δ^4 function ensures energy-momentum conservation. In the general case where the final states p_1,p_2 are off shell, A represents the full positive-energy spectral function. In the quasiparticle approximation A reduces to the on-shell condition

$$A(p)=2\pi\delta(p^{*2}-M^{*2})2\Theta(p_0^*). \tag{23}$$

Thus the spectral function fulfills the sum rule

$$\int\frac{dp_0}{(2\pi)}A(p)=\frac{1}{E^*(\mathbf{p})}. \tag{24}$$

Here we choose spectral functions of a Breit-Wigner form

$$A(p)=2\pi\frac{1}{\pi}\frac{2p_0\Gamma}{(p^{*2}-M^{*2})^2+(p_0\Gamma)^2}. \tag{25}$$

Thus A satisfies the sum rule and in the zero-width limit $\Gamma\mapsto 0$ the quasiparticle approximation (23) is recovered. In the two-particle c.m. frame the integral (22) can easily be evaluated. The total cross section is then given by

$$d\sigma=\frac{2M^{*4}}{\pi^4\sqrt{s^*(s^*-4M^{*2})}}d\Omega\int p^2dp|T(p,q,\theta)|^2 \times\int\frac{dp_0(2E^*(\mathbf{q})-p_0)p_0\Gamma^2}{(\{[2E^*(\mathbf{q})-p_0]^2-(p^2+M^{*2})\}^2+[2E^*(\mathbf{q})-p_0]^2\Gamma^2)[(p_0^2-p^2-M^{*2})^2+p_0^2\Gamma^2]}, \tag{26}$$

which reduces to expression (10) in the zero-width limit. As discussed in [3] the width Γ is determined by the imaginary part of the self-energy,

$$\Gamma=-\frac{M^*}{E^*(\mathbf{p})}\mathrm{Im}\,\Sigma_s(\rho,\mathbf{p})+\mathrm{Im}\,\Sigma_0(\rho,\mathbf{p}), \tag{27}$$

and depends on the density and momentum. In the present approach Γ follows from the imaginary part of the T matrix. It can, however, only serve as an estimate for the full particle width inside the medium. As discussed in Sec. II the Bethe-Salpeter equation is solved in the quasiparticle approximation. For the determination of the T matrix this treatment is justified since the condition $\Gamma\ll E_{\mathrm{s.p.}}=E^*-\Sigma_0$ is readily fulfilled. However, since the standard Brueckner-Hartree-Fock (BHF) approach accounts only for the particle-particle correlations of the Brueckner hole-line expansion $\mathrm{Im}\,\Sigma$ vanishes for momenta below the Fermi surface due to Pauli blocking. Long-range correlations which are usually treated in random-phase-approximation-type (RPA-type) approaches by a ladder summation in the particle-hole channel contribute to the spectral width [36], but are not taken into account in the standard Brueckner-Hartree-Fock approach. RPA correlations lead further to a depletion just below the Fermi surface and an occupation of states above the Fermi surface. Thus, the Dirac-BHF (DBHF) results for Γ do not represent the full width but give a reliable estimate only at momenta well above the Fermi surface where particle-particle correlations can be regarded as the dominant contributions to Γ. In the considered density and energy range Γ ranges from about 10 MeV at $0.5\rho_0$ to more than 40 MeV at $3\rho_0$ as the outcome of the present DBHF calculations [13].

Thus, the cross sections shown in Figs. 11 (np) and 12 (pp) give an estimate for the off-shell dependence of the total cross section. For this purpose we choose two typical values for Γ which cover the range of spectral width in nuclear matter as is predicted by DBHF calculations, i.e., $\Gamma=10$ MeV and 40 MeV. The present results are obtained with a constant, i.e., momentum-independent, Γ. For a better comparison of the various densities the cross sections are shown as a function of $2\mathbf{q}^2/M$ which corresponds in the vacuum to the laboratory energy. It can be seen from Figs. 11 and 12 that the off-shell dependence of the total cross section is moderate. The averaging over the Breit-Wigner distributions leads to significantly smaller off-shell effects than are seen in the scattering amplitudes. Compared to the on-shell value the cross sections are generally reduced, in the case of $\Gamma=40$ MeV by about 15–20 %. At small nuclear densities this reduction is most pronounced at low momenta whereas at higher momenta there is no sizable effect. At large densities the reduction is more pronounced at high momenta. Only for large values of $\Gamma\simeq 100$ MeV (not shown here) can a reduction of the cross section of more than 50% be reached. Differences in the off-shell structure of the NN interaction, e.g., using Bonn C, do not lead to essentially different results. This is consistent with the observations made in Ref. [21] where it has been demonstrated that the on-shell cross sections are not much affected by the use of different parametrizations like Bonn B or C.

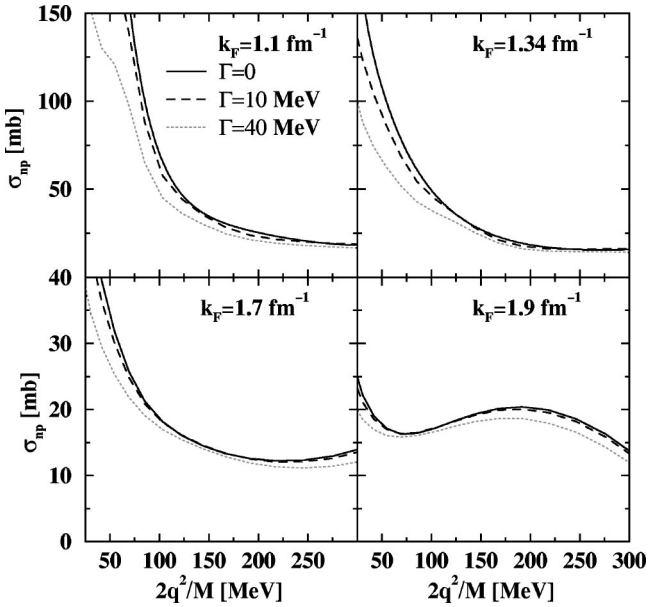

FIG. 11. Total np cross section at various densities as a function of $2\mathbf{q}^2/M$. The quasiparticle approximation ($\Gamma=0$) is compared to the case where the final states have a finite spectral width of $\Gamma=10$, 40 MeV.

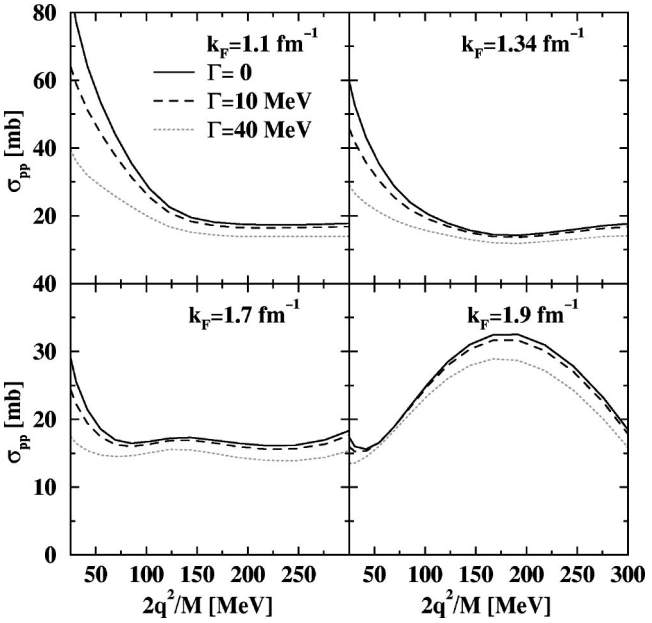

FIG. 12. Total pp cross section at various densities as a function of $2\mathbf{q}^2/M$. The quasiparticle approximation ($\Gamma=0$) is compared to the case where the final states have a finite spectral with of $\Gamma=10$, 40 MeV.

V. SUMMARY

In the present work we investigated the in-medium nucleon-nucleon cross section within the relativistic (Dirac) Brueckner-Hartree-Fock approach. We considered both on-shell scattering and the more general case where the final momenta are allowed to be off energy shell. The in-medium cross sections can serve as input for transport calculation of heavy ion collisions. Information on the off-shell dependence of the scattering amplitudes is required when one intends to go beyond the quasiparticle approximation in order to obtain a more realistic description of transport phenomena for particles with finite width. In a dense hadronic environment created, e.g., in heavy ion collisions also ''stable particles'' like nucleons acquire a finite spectral width. Throughout this work we applied the Bonn A potential as the nucleon-nucleon interaction since this potential yields the most reasonable saturation properties for nuclear matter.

Concerning the on-shell scattering we find a qualitative agreement with the previous investigations of Li and Machleidt [21], however, less reduced in-medium cross sections at low energies. The reason therefore lies in the fact that we account for modifications of the optical theorem due to the presence of the medium which have been neglected in the approximation made in [21]. In the np cross section an additional low-density enhancement appears which can be interpreted as the precursor of a superfluid state. The present approach was then extended to the case where incoming and outgoing momenta of the scattered nucleons can vary independently and—due to energy-momentum conservation—the final states are off energy shell. The resulting T-matrix elements or transition amplitudes show a strong variation around the on-shell point. The shape of the transition amplitudes depends, however, mainly in a symmetric way on the incoming and outgoing momenta. The fact that the final states are off shell and the incoming ones on shell plays thereby a minor role. This allows one to approximate the half-off-shell matrix elements in a suitable way by their on-shell values. Such an approximation works well at moderate nuclear matter densities but at large densities precise knowledge of the amplitudes is required. In a conservative estimate finite width effects lead to a reduction of the total cross sections by about 20% compared to the on-shell scattering. Off-shell effects are more pronounced at larger nuclear densities.

[1] P. C. Martin and J. Schwinger, Phys. Rev. **115**, 1342 (1959).
[2] S. R. de Groot, W. A. van Leeuwen, and C. G. van Weert, *Relativistic Kinetic Theory* (North-Holland, Amsterdam, 1980).
[3] W. Botermans and R. Malfliet, Phys. Rep. **198**, 115 (1990).
[4] J. Jaenicke, J. Aichelin, N. Ohtsuka, R. Linden, and A. Faessler, Nucl. Phys. **A536**, 201 (1992).
[5] D. T. Khoa, N. Ohtsuka, M. A. Matin, A. Faessler, S. W. Huang, E. Lehmann, and R. K. Puri, Nucl. Phys. **A548**, 102 (1992).
[6] Y.-M. Zheng, C. M. Ko, B.-A. Li, and Bin Zhang, Phys. Rev. Lett. **83**, 2534 (1999).
[7] C. J. Horowitz and B. D. Serot, Nucl. Phys. **A464**, 613 (1987).
[8] B. ter Haar and R. Malfliet, Phys. Rep. **149**, 207 (1987).
[9] C. Nuppenau, Y. J. Lee, and A. D. MacKellar, Nucl. Phys. **A504**, 839 (1989).
[10] R. Brockmann and R. Machleidt, Phys. Rev. C **42**, 1965 (1990); nucl-th/9612994.
[11] L. Sehn, C. Fuchs, and A. Faessler, Phys. Rev. C **56**, 216 (1997).
[12] C. Fuchs, T. Waindzoch, A. Faessler, and D. S. Kosov, Phys. Rev. C **58**, 2022 (1998).
[13] T. Gross-Boelting, C. Fuchs, and A. Faessler, Nucl. Phys. **A648**, 105 (1999).
[14] R. Machleidt, in *Advances in Nuclear Physics*, edited by J. W. Negele and E. Vogt (Plenum, New York, 1989), Vol. 19, p. 189.
[15] B. D. Serot and J. D. Walecka, in *Advances in Nuclear Physics*, edited by J. W. Negele and E. Vogt (Plenum, New York, 1986), Vol. 16, p. 1.
[16] M. Schmidt, G. Röpke, and H. Schulz, Ann. Phys. (N.Y.) **202**, 57 (1990).
[17] T. Alm, G. Röpke, and M. Schmidt, Phys. Rev. C **50**, 31 (1994).
[18] B. ter Haar and R. Malfliet, Phys. Rev. C **36**, 1611 (1987).
[19] R. Malfliet, Prog. Part. Nucl. Phys. **21**, 207 (1988).
[20] C. Fuchs, L. Sehn, and H. H. Wolter, Nucl. Phys. **A601**, 505 (1996).
[21] G. Q. Li and R. Machleidt, Phys. Rev. C **48**, 1702 (1993); **49**, 566 (1994).
[22] Yu. Ivanov, J. Knoll, and D. N. Voskresensky, Nucl. Phys. **A657**, 413 (1999).
[23] P. Henning, Phys. Rep. **253**, 235 (1995).

[24] R. Fauser and H. H. Wolter, Nucl. Phys. **A584**, 604 (1995).
[25] K. Morawetz and H. S. Köhler, Eur. Phys. J. A **4**, 291 (1999).
[26] S. Leupold, Nucl. Phys. **A672**, 475 (2000); J. Lehr, M. Effenberger, H. Lenske, S. Leupold, and U. Mosel, Phys. Lett. B **483**, 324 (2000).
[27] W. Cassing and S. Juchem, Nucl. Phys. **A665**, 377 (2000); **A672**, 417 (2000); **A677**, 445 (2000).
[28] K. Morawetz, V. Spicka, P. Lipavsky, G. Kortemeyer, Ch. Kurts, and R. Nebauer, Phys. Rev. Lett. **82**, 3767 (1999); K. Morawetz, P. Lipavsky, V. Spicka, and N.-H. Kwong, Phys. Rev. C **59**, 3052 (1999).
[29] G. E. Brown and A. D. Jackson, *The Nucleon Nucleon Interaction* (North-Holland, Amsterdam, 1976).
[30] K. Erkelenz, Phys. Rep. **13**, 191 (1974).
[31] M. I. Haftel and F. Tabakin, Nucl. Phys. **A158**, 1 (1970).
[32] M. Trefz, A. Faessler, and W. H. Dickhoff, Nucl. Phys. **A443**, 499 (1985).
[33] M. Rose, *Elementary Theory of Angular Momentum* (Wiley, New York, 1957).
[34] P. F. Shepard *et al.*, Phys. Rev. D **10**, 2735 (1974).
[35] B. E. Vonderfecht, C. C. Gearhart, W. H. Dickhoff, A. Polls, and A. Ramos, Phys. Lett. B **253**, 1 (1991).
[36] H. Müther and A. Polls, Prog. Part. Nucl. Phys. **45**, 243 (2000).